Combustion of sewage sludge: Kinetics and speciation of the combustibles

Jonas Wielinski[a,b], Christoph Müller[c], Andreas Voegelin[a], Eberhard Morgenroth[a,b], Ralf Kaegi[a,*]

[a] Eawag, Swiss Federal Institute of Aquatic Science and Technology, 8600 Dübendorf, Switzerland

[b] ETH Zürich, Institute of Environmental Engineering, 8093 Zürich, Switzerland

[c] ETH Zürich, Institute of Energy Technology, 8092 Zürich, Switzerland

* Corresponding author, e-mail: ralf.kaegi@eawag.ch, fax: +41 58 765 5802, Eawag, Überlandstrasse 133, 8600 Dübendorf, Switzerland

This document is the accepted manuscript version of the following article: Wielinski, J., Müller, C., Voegelin, A., Morgenroth, E., & Kaegi, R. (2018). Combustion of sewage sludge: kinetics and speciation of the combustible. Energy and Fuels. https://doi.org/10.1021/acs.energyfuels.8b02106

Abstract: Combustion of sewage sludge has become a viable route for sewage sludge management especially as the agricultural use of sewage sludge has become increasingly difficult due to more stringent requirements on the quality of the sewage sludge. Combustion of digested sewage sludge in dedicated mono-combustion facilities is advantageous, as it substantially reduces the volume of the sludge and still allows for a recovery of phosphorus from the sewage sludge ash at a later stage. Despite increasing amounts of sewage sludge being combusted, our knowledge on the respective combustion kinetics is still fragmentary. The goal of this study was, therefore, to identify the major combustion reactions of sewage sludge, assess their Arrhenius parameters (activation energy, pre-exponential factor) and assign suitable reference compounds to the individual reactions. For that purpose, experiments were conducted using a thermogravimetric analyzer (TGA). With matrix inversion, we identified 10 individual reactions. Despite the apparent kinetic compensation most likely caused by insufficient precision of the TGA temperature setting, we were able to relate the major reactions of sewage sludge combustion to the combustion of individual reference compounds. In addition to cellulose and lignin which dominated the weight loss with 35% and 20% respectively, hemicellulose, xylan, alginate, and calcite were identified. The dominant fraction of cellulose is consistent with recent studies identifying cellulose mainly originating from toilet paper as a major constituent in wastewater. As the identified model compounds explain more than 80% of the total weight loss observed, our approach allows a rough speciation of the combustible of sewage sludge based on TGA experiments.

Keywords: Sewage sludge; Combustion; Kinetics; Thermogravimetry

1 Introduction

Wastewater treatment plants (WWTPs) are designed to protect water resources by removing nutrients, contaminants and suspended solids from the wastewater. Following a series of biological and physical processes in distinct reactors treated wastewater is discharged to surface waters. Sewage sludge, a by-product of wastewater treatment, is usually digested for stabilization and further processing [1]. In Europe, roughly 20% of the digested sewage sludge is incinerated [2]. In Switzerland, the application of sewage

sludge in agriculture was banned in 2006 and sewage sludge is exclusively incinerated [3]. Also in the Netherlands, combustion is the major disposal pathway for sewage sludge [2]. In Germany, sewage sludge is to a large extent incinerated, preferentially in dedicated mono-combustion fluidized-bed reactors [2-4]. In the United States and Japan, approximates 25% and 55% of the sewage sludge are combusted[5]. Besides reducing the volumes of sewage sludge, the combustion in dedicated fluidized-bed reactors additionally offers the advantage of subsequent phosphate recovery from the sewage sludge ashes, which is impossible when sewage sludge is co-incinerated with municipal solid waste [6].

Primary sewage sludge consists of larger particles which are separated from the wastewater during primary treatment in a sedimentation tank. Secondary (activated) sludge is produced during the activated sludge process (mostly consisting of a combination of nitrification and denitrification reactors) and is mainly composed of cell tissue and extracellular polymeric substances [1]. For anaerobic digestion, a mixture of primary and secondary (excess) sludge is used. Thus, sewage sludge can be considered as complex waste fuel with a calorimetric value of about 10.5 MJ/kg dry matter [5]. Cellulose fibers mainly from toilet paper likely represent a major constituent in wastewater and attempts to recover or eliminate cellulose fibers during wastewater treatment have recently been presented [7-8]. High concentrations in the influent and only incomplete degrading of the cellulose fibers during anaerobic digestion suggest that cellulose is also present in considerable amounts in the digested sludge [7, 9].

Numerous studies have investigated the kinetics of sewage sludge pyrolysis [10-16], referring to incineration in the absence of oxygen. However, the kinetics of sewage sludge combustion (presence of oxygen) have only received limited attention [10, 17]. Hernandez et al., investigated the incineration of sewage sludge by differential thermogravimetry (TG) using N_2, CO_2 and synthetic air [17]. Five reactions with reaction orders close to one were used to describe the overall devolatilization and combustion of sewage sludge.

In this paper, we present results from a series of TG experiments aimed to study the combustion of municipal digested sewage sludge. We used an evaluation algorithm that allows the identification of a set of first-order reactions based on objective criteria [18]. We identified the main reactions occurring during

sewage sludge combustion and characterized these reactions in terms of their kinetic parameters. Based on literature data, we assigned model compounds to the identified reactions and determined the fractions of the total conversion associated with these reference compounds. This approach allowed us to roughly assess the speciation of combustible in digested sewage sludge based on TG experiments.

2 Evaluation of TG experiments

The rate constants of combustion reactions of solid fuel can generally be described using the Arrhenius equation

$$k(T) = A \exp(-\frac{E}{RT}) \quad (1)$$

with k representing the reaction rate constant, E the activation energy, A the pre-exponential factor, T the temperature and R the universal gas constant [19]. The change of the extent of fuel conversion α over time t depends on the reaction model f(α), the reaction rate constant k(T) and a gas pressure dependent function h(p).

$$\frac{d\alpha}{dt} = f(\alpha)k(T)h(p) \quad (2)$$

The extent of fuel conversion runs from zero to one. The pressure dependency was neglected in the following considerations, as all experiments were conducted at constant partial pressures of oxygen. A function $g(\alpha)$ can be defined based on integrating the inverse of $f(\alpha)$:

$$g(\alpha) \equiv \int_0^\alpha \frac{1}{f(\alpha)} d\alpha \, . \quad (3)$$

The function $g(\alpha)$ is the integrated form of the reaction model. Equation 2 can be rearranged by separation of variables. Therefore, the combination of equations 1, 2 and 3 leads to:

$$g(\alpha) = A \int_0^t \exp(\frac{-E}{RT(t)}) \, dt. \quad (4)$$

A more detailed derivation of equation 4 is given in Supporting Information (SI). A selection of reaction models (g(α)) can be found in Burnham (2017) [20].

In our study the identification and characterization of individual combustion reactions was based on an algorithm developed for the evaluation of TG results obtained from the pyrolysis of sewage sludge and other complex fuels [18]. The algorithm is based on a matrix inversion, and requires that two TG experiments are conducted with the same materials but at different heating rates. This allows the identification of individual first-order combustion reactions and their corresponding kinetic triplets (activation energy E, the pre-exponential factor A and the relative contribution of the individual reaction to the total reacting solid f_0). For a detailed discussion of the algorithm and its underlying mathematics, the reader is referred to the work of Scott et al. (2006) [18]. The integrated first-order reaction model is given in equation (5):

$$g(\alpha) = -\ln(1-\alpha). \quad (5)$$

Thermograms, determined by TG can be normalized by $W(t) = (M(t) - M_{\mathrm{end}})/(M_0 - M_{\mathrm{end}})$ with $W(t)$ representing the normalized weight of the total reacting solid, $M(t)$ the weight at time point t, M_0 the weight at the beginning of the experiment and M_{end} the weight at the end of the experiment. The normalized weight relates to the extent of conversion by $W(\mathrm{t}) = 1 - \alpha$. Based on the number of reactions n and their kinetic parameters (E, A, f_0), the modeled normalized weight $\widehat{W(t)}$ can be calculated using equation 6 which results from the combination of equation 4 and 5 and the relation between $W(t)$ and α.

$$\widehat{W(t)} = \sum_{i=1}^{n} f_{i,0}\, exp\left(-A_i \int_0^t exp\left(\frac{E_i}{RT(t)}\right) dt\right) \quad (6)$$

With $\mathrm{i} = 1$ to n reactions occurring during an experiment running from time point zero to t. In theory, the sum of all fractions $f_{i,0}$ equals one, but in practice, slight deviations from one are observed. The integration over time (dt) can be replaced by an integration over temperature (dT) using a constant heating rate $B = dT/dt$. The measured, normalized weights $W(t)$ can be compared to the modeled, normalized weights $\widehat{W(t)}$, so that

$$W(t) \cong \widehat{W(t)} = \sum_{i=1}^{n} f_{i,0} \exp\left(-\frac{A_i}{B}\int_{T_0}^{T'} \exp\left(\frac{E_i}{RT(t)}\right)\, dT\right). \quad (7)$$

The algorithm has already been applied successfully to identify and characterize reactions from synthetic data and reactions based on TG results obtained from the pyrolysis of sewage sludge [16]. In the following, this algorithm will be referred to as TGA evaluation algorithm. The TGA evaluation algorithm has, to the best of our knowledge, not yet been applied to retrieve the kinetic parameters of the combustion of digested sewage sludge.

3 Materials and Methods

Digested sewage sludge was collected from a pilot WWTP at Eawag, Switzerland at three different time points (January 1st 2017, June 15th 2017 and July 3rd 2017 for P1 P2 and P3, respectively). One sludge sample (P1) was investigated in detail and two further sludge samples (P2, P3) were collected to reveal the variability of the recorded thermograms resulting from seasonal variations of the digested sludge. The sludge was freeze dried, milled in a ball mill with 17 Hz for 4 min (MM 400, Retsch, Switzerland) and sieved to 125 µm < d < 250 µm. Samples were transferred to 1.5 mL Eppendorf tubes and stored in the dark at room temperature. Powdered and sieved sludge samples (5 to 8 mg) were added to 70 µl alumina (Al_2O_3) crucibles, heated in a TGA (TGA DSC1, Mettler Toledo, USA) and the weight loss was recorded at a sampling rate of 1 Hz. For the extraction of the kinetics parameters of individual combustion reactions, thermograms were recorded from room temperature to 900°Cat temperature ramps of 10 and 20K/min. Additional thermograms were recorded at heating rates of 1 and 100 K/min to investigate the impact of the heating rates on the apparent kinetic compensation. All experiments included a 5 min drying step at 105 °C. Blank runs with empty crucibles were conducted to compensate for buoyancy. A gas flow of 25 mL/min of synthetic air (80% N_2, 20% O_2) created an oxidizing atmosphere during the experiments. The balance was protected by a 25 mL/min N_2 purge gas flow. The recorded data (sample temperature, sample weight, heat flow over the furnace) was exported as a text file using the Mettler Toledo Star software and imported into Matlab. The discrete data were transferred into a spline for further processing. Carbon contents were measured on a Euro EA - CHNSO Elemental Analyser (HEKAtech,

Germany). For that purpose, 5 to 10 mg of dried sewage sludge or ash from the TGA experiments were mixed (1:1) with a vanadium oxide catalyst and wrapped in tin foil. Four replicates were conducted with the dried sludge to assess the variability of the carbon contents in the sludge samples. Inorganic carbon content was assessed using a titration CO_2-coulometer (UIC Inc., Joliet, USA). Major characteristics and number of repetitions conducted with each sludge samples are given in Table 1.

Table 1: Total carbon, inorganic carbon, ash content and the number of repetitions of the TGA experiments of P1, P2 and P3.

Sample name	Carbon content, % (mean ± std or single value)	Inorganic carbon content, %	Ash content, % (mean ± std)	TGA repetitions with 10 and 20°C/min heating ramps
Sewage sludge P1	35.5 ± 0.1 (n = 4)	1.85	29.9 ± 0.7 (n = 18)	9
Sewage sludge P2	34.7	0.97	27.7 ± 0.6 (n = 6)	3
Sewage sludge P3	not determined	not determined	24.7 ± 0.2 (n = 2)	1

4 Results and discussion

4.1 Combustion of sewage sludge

The normalized thermograms (Figure 1a) of the replicates from the same sludge samples (replicates of P1 and P2) look very similar. Larger deviations were observed between the normalized thermograms of the three sludge samples (Figure 1). Based on TG results, the combustion of sewage sludge was divided into three phases (Figure 1). The devolatilization rate of all sludge samples increased progressively until about

250 °C (Figure 1b). After 250 °C, the increase in weight change lessens, which is reflected by a shoulder of the first derivative (Figure 1b). The change of weight loss of all replicates reaches a maximum towards the end of phase 1 at roughly 325 °C (Figure 1b). In phase 2, the change of the weight loss first decreases, but then remains roughly constant for P1 and P2. However, the first derivative of the weight loss of sample P3 shows a peak towards the end of phase 2. At the end of phase 2, the rate of weight loss decreases sharply to almost zero. At the beginning of phase 3, the weight loss remains close to zero and raises again at 650 °C (P1) and 620 °C (P2 and P3). In a comparable TGA study of the combustion of sewage sludge three combustion phases with slightly different temperature ranges compared to the present study were identified [17]. The first phase in that study describing the evaporation of residual water in the sludge is not displayed in the present study. Differences observed at higher temperatures most likely result from different sludge compositions used in the two studies. Furthermore, in this study, we observed an inorganic transformation phase (phase 3), which was not reported by Hernandez et al. [17]. The three sewage samples (P1 – P3) of this study were similar as they all exhibited the three distinct combustion phases. However, there are significant differences within the individual combustion phases, especially phase 2. During phase 1 (devolatilization), P1 - P3 mostly followed the same trend. Only towards the end of phase 1, the curves diverge and the weight change is in the following order: P3 < P1 < P2. In phase 2 the curves of P1 and P2 are straight and run parallel, but P3 exhibits a convex shape. This convex shape is reflected by a peak in the first derivative of P3 at the end of phase 2. During phase 3, the relative weight which is converted is rather small for P2 and P3 but considerable for P1.

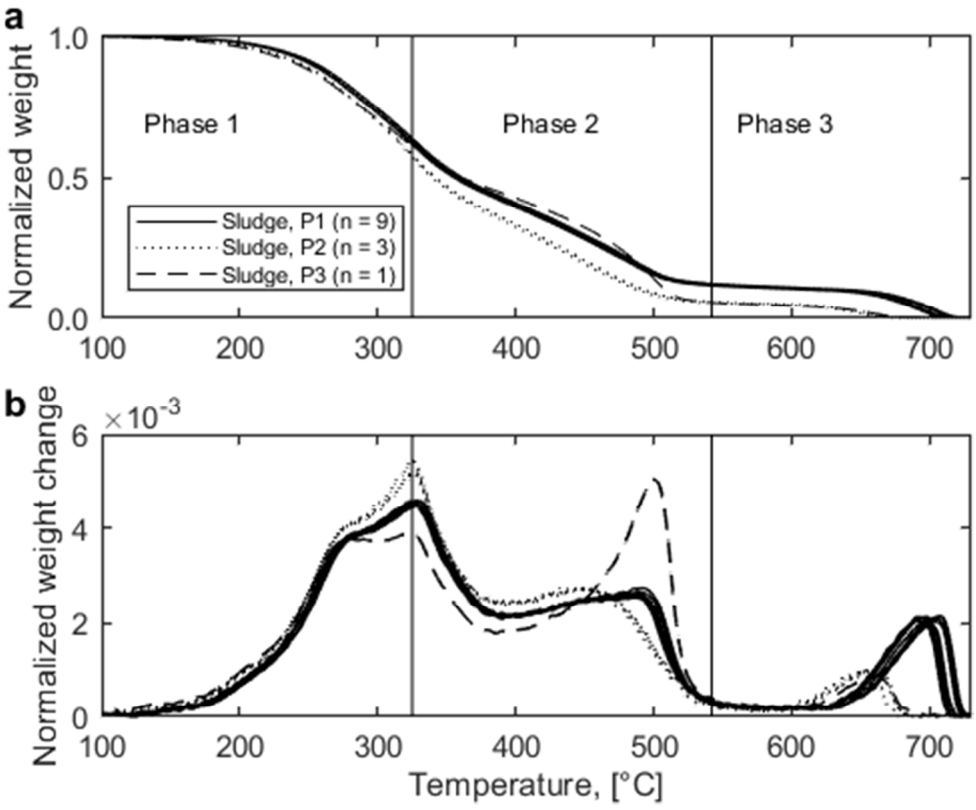

Figure 1a: Thermograms (normalized weight versus temperature) from sludge P1 (nine replicates), sludge P2 (three replicates) and sludge P3 (one experimental run) recorded with a heating rate of 10 K/min. Three combustion phases were identified: phase 1 (105 – 325 °C), phase 2 (325 – 540 °C) and phase 3 (540 – 730 °C). Figure 1b: Change of normalized weight (first derivative) versus temperature.

4.2 Major combustion reactions of digested sewage sludge

Nine replicates, each consisting of two experiments with heating ramps of 10 and 20 K/min were conducted with the sludge sample P1. Ten individual reactions were identified by applying the TGA evaluation algorithm to this dataset (Table 2 and Figure 2). To assess the performance of the TGA evaluation algorithm, we used the extracted kinetic data of the identified reactions to construct modeled thermograms (e.g. Figure 3, reaction 1 to 10 or Figure S1, colored lines). The modeled TGs were reprocessed using the TGA evaluation algorithm to obtain kinetic parameters and number of reactions. Kinetic parameters extracted from the measured data given in blue circles and extracted kinetic parameters from modeled curves given by red squares (Figure S2) are in good agreement. These results demonstrate

that the TGA evaluation algorithm - assuming of n first-order reactions – reliably extracts the number of reactions and their corresponding kinetic parameters at the given level of complexity of the sludge samples. However, as the evaluation algorithm represents an interpretation of the measured thermograms, the results do not prove the existence of the identified reactions.

The TGA evaluation algorithm was applied to the combustion of digested sewage sludge and the modeled, normalized weight curve $\widehat{W(t)}$ only showed minor deviations from the measured, normalized weight (W(t)) (Figure S1) with an $r^2 = 0.8755 \pm 0.0025$ (n = 9). An average curve, comprised of the mean values from all 9 replicate thermograms even resulted in a squared correlation very close to 1.0 ($r^2 = 0.99992$). The contributions of the individual reactions to the overall weight loss is displayed in Figure 3. Results from multiple repetitions of P1 are displayed in a Constable plot showing the natural logarithm of A versus E (Figure 4, only reactions associated with weight changes > 2% are displayed and used for further evaluations). Each color represents one replicate. The diameter of the circles relates to f_0; larger circles indicate larger fractions. A, E and f_0 were determined for each replicate individually resulting in 9 circles for each reaction. The circles associated with individual reactions exhibit a considerable spread, but always project along a straight line. The spread in E can be related to either the selection of an inappropriate combustion model ($f(\alpha)$) [21], random experimental errors [22], or (apparent) kinetic compensation [23-24]. A linear relationship between E and the natural logarithm of A is referred to as kinetic compensation effect, isokinetic effect or enthalpy-entropy compensation, which, however, are very different effects [23]. Different explanations for these effects have been reported in the scientific literature, but no consensus has been reached concerning the origins and underlying mechanisms. Liu and Guo provide a comprehensive review on this topic [23]. Apparent kinetic compensation resulting from random experimental and systematic errors are discussed in Barrie and we based our assessments of the (apparent) kinetic compensation on these two publications [22], [24]. The source and the implications of the considerable variation in E and / or A will be addressed in detail in the next section.

In a study on pyrolysis of digested sewage sludge, the TGA evaluation algorithm identified 18 reactions that accounted for approximately 85% of the weight loss [16]. The large number of reactions can be explained by the complex matrix of digested sludge. In contrast, the pyrolysis of activated (undigested) sludge was reported to consist of only 8 reactions. The lower number of reactions identified in this study compared to the higher number of reactions reported by Scott et al. is likely caused by the less complete digestion of the sludge in our pilot system compared to a full scale system [16]. Reactions 1 to 7 essentially accounting for phase 1 can be assigned to the devolatilization of readily bio-degradable compounds. Reactions 8 and 9 in phase 2 represent the burning of natural organic matter, char and other relatively recalcitrant organic molecules [12-13]. Reaction 10, representing phase 3, corresponds to the degassing or transformation of inorganic substances most likely carbonates (Figure 2) [10].

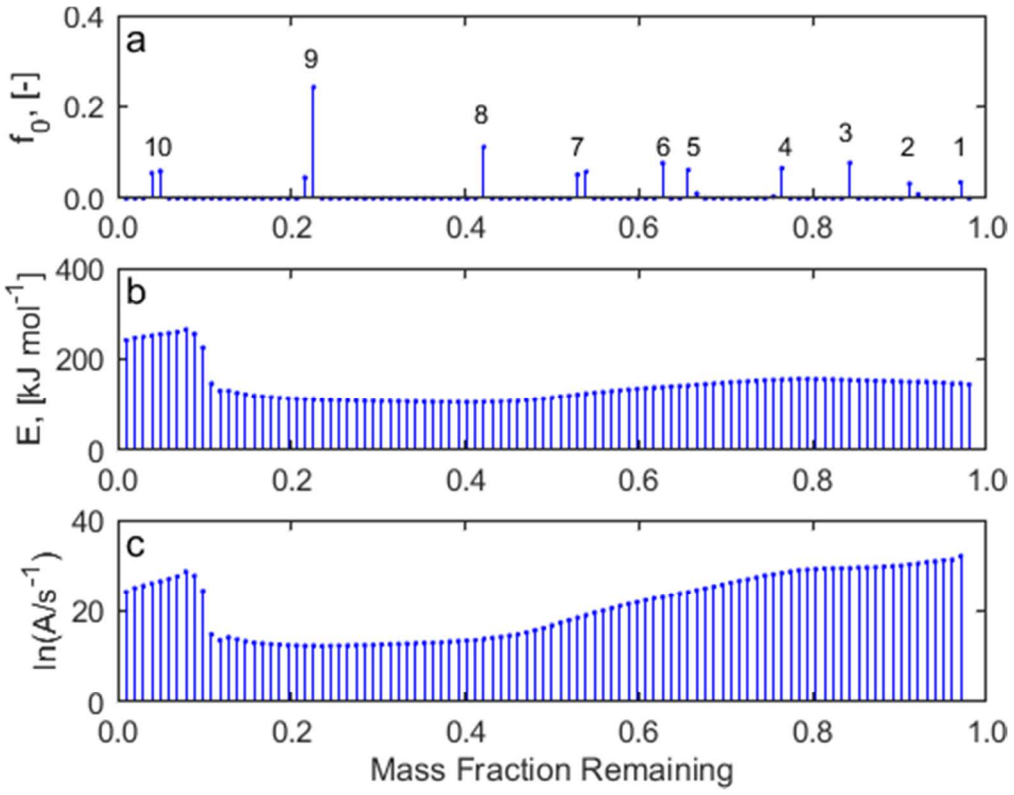

Figure 2: Fractions (f_0) of total conversion associated with identified reactions, and change of activation energy (E) and pre-exponential factor (A) with increasing temperature. Figure 2a: A reaction is observed

every time f_0 is larger than zero. If f_0 is larger than zero in two consecutive conversion spots they can be merged into one reaction [18]. The numbers 1 to 10 refer to identified reactions. Figure 2b shows the evolution of the E and Figure 2c shows the development of A. The experimentally induced heating proceeds from right to left.

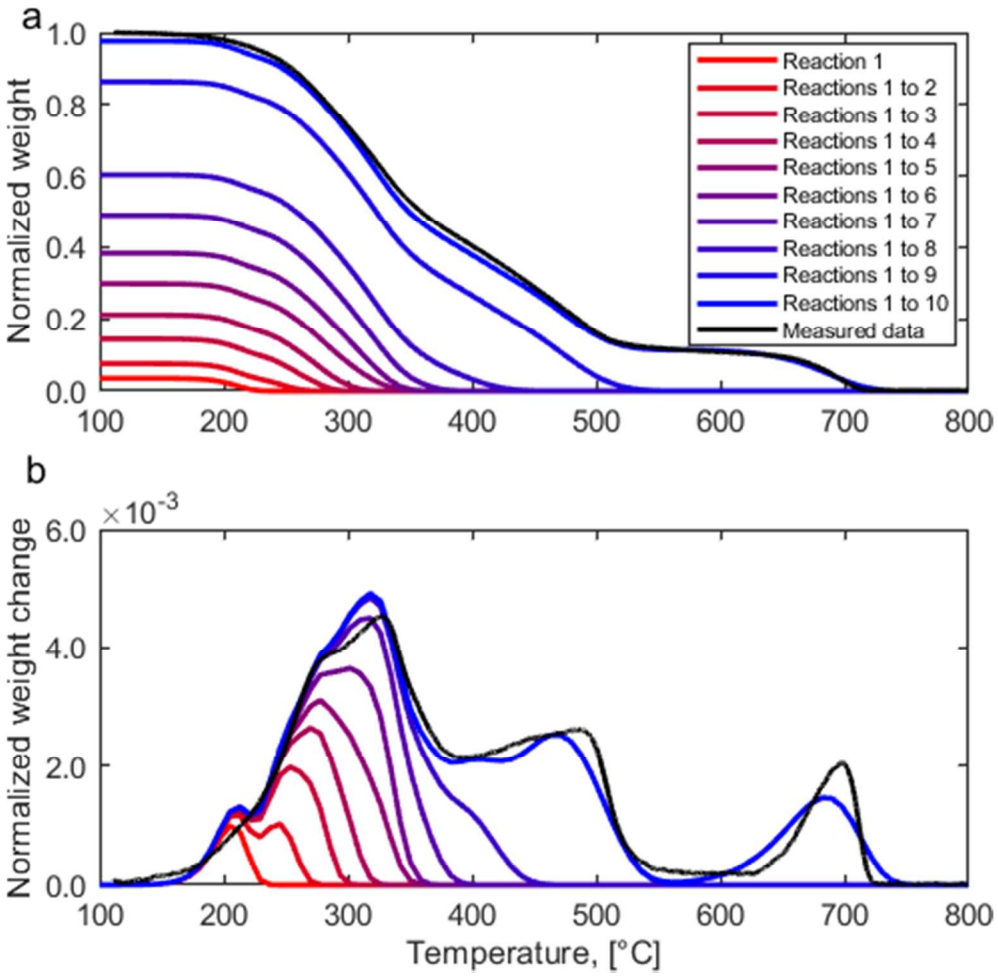

Figure 3a: Normalized weight (and fraction) of the identified reactions and the measured data versus the temperature of a 10 K/min heating rate experiment. Different colors indicate the superposition of an increasing amount of reactions. Figure 3b: Normalized weight change of the identified reactions.

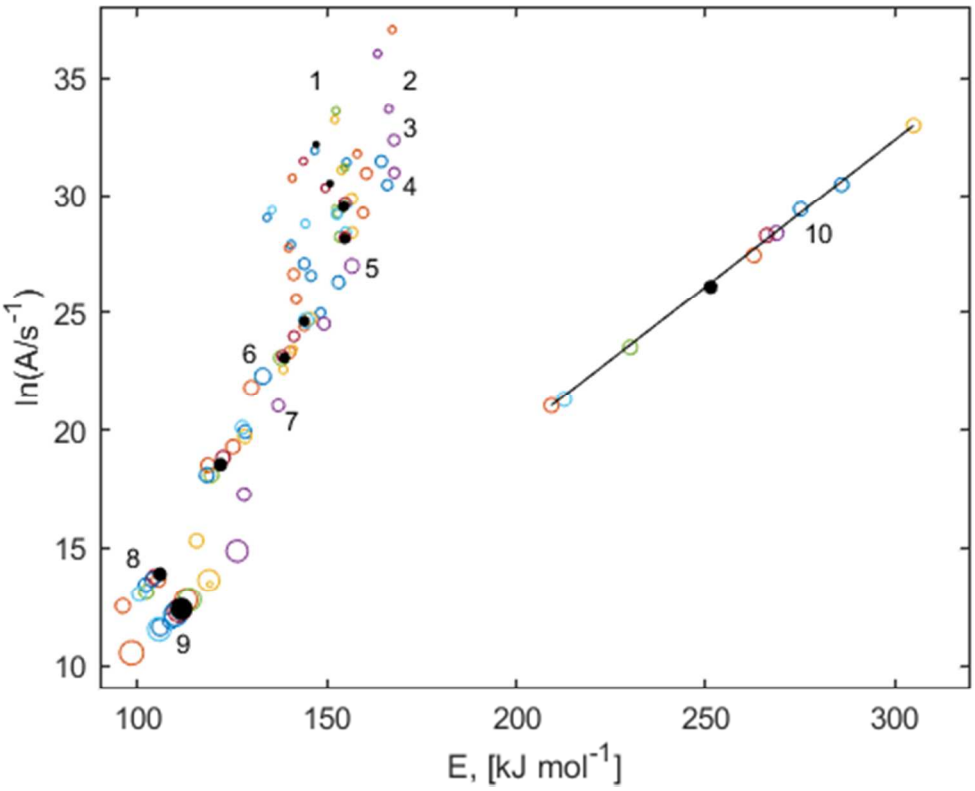

Figure 4: Results of 9 replicates of the TG experiment using P1. Each dot represents a reaction which is characterized by an activation energy (E, x-axis), a pre-exponential factor (A, y-axis) and a weight fraction (f_0, size of the dot). Each color represents one replicate and the filled black dots represent the results of the evaluation of the average thermogram. The numbers indicate the "reaction number" and correspond to those in Figure 2a.

Table 2: Kinetic parameters (E (activation energy), A (pre-exponential factor), f_0 (fraction of the total conversion)) obtained for the average curve of all replicates of P1 and comparable reactions from the literature. *Reactions taken from [17].

Reaction number	E [kJ/mol]	Ln(A) [1/s])	f_0 ($\sum = 0.98$)	r^2 (linear regression through all replicates of a reaction)	Harmonic mean temperature of the reaction ($\overline{T_{\mathrm{hm}}}$, [K])	Comparable reaction(s)
1	148.3	32.45	0.0347	0.9992	500.9	None identified
2	151.3	30.43	0.0402	0.9967	536.8	• (Hemicellulos reaction 1 [42]) • (Xylan reaction 1 [42])
3	154.7	29.58	0.0683	0.9980	563.2	• Sewage sludge combustion: Reaction 1* • Alginate [33]
4	155.6	28.42	0.0680	0.9964	600.0	• Sewage sludge combustion: Reaction 2*
5	147.0	25.12	0.0871	0.9943	610.7	None identified
6	139.5	23.23	0.0848	0.9720	763.1	• Sewage sludge combustion: Reaction 3* • Cellulose volatilization [43] • Cellulose volatile oxidation [44] • Xylan reaction 2 [42]
7	124.7	19.22	0.1068	0.9741	751.6	• Sewage sludge combustion: Reaction 4* • Cellulose reaction 1 [45] • Hemi cellulose Reaction 2 [42]
8	106.4	13.98	0.1132	0.9962	803.8	• Cellulose char oxidation [46]
9	111.2	12.43	0.2602	0.9982	761.6	• Sewage sludge combustion: Reaction 5* • Lignin reaction 2 [45] • Cellulose reaction 2 [45]
10	256.7	26.89	0.1135	0.9990	957.5	• Calcite [34]

4.3 Determination of confidence regions for the kinetic parameters

We investigated whether the variations in E and A can be attributed to random experimental errors or systematic errors. Thereafter, we elaborate on the most likely source of the apparent kinetic compensation observed in our experiments.

It is important to distinguish between a spread of the data which is caused by measurement uncertainties (random and systematical experimental errors) and a spread which has a chemical and/or physical origin (physicochemical effects), resulting from e.g. progressive deactivation of a catalyst surface [22, 24-26]. We determined confidence ellipses which define the extent of the spread of E caused by random experimental errors. For that purpose, we calculated the square-root of the eigenvalues (λ_1 and λ_2) of the variance-covariance matrix [22, 27-28].

$$\lambda_1 = \frac{1}{m}\left(\frac{\rho^2}{1-\rho^2}\right)\left(T_{hm}^2 + 1\right) \quad (8)$$

$$\lambda_2 = \frac{1}{m} \quad (9)$$

With m representing the number of data points included for a linear regression, ρ representing the extent of correlation between E and ln(A) and $T_{\mathrm{hm}} = n/\sum_{\mathrm{i}=1}^{\mathrm{n}} \frac{1}{T_{\mathrm{i}}}$ representing the harmonic mean of the temperatures at which the conversions occur. λ_1 and λ_2 are the lengths of the semi-major and semi-minor axis of the confidence ellipses, respectively. The orientation Θ of the ellipses relates to the inverse of the harmonic mean temperature ($\tan\Theta = 1/(RT_{\mathrm{hm}})$). If the projections of the experimental results (E and ln(A)) plot within the confidence ellipses of each other the observed spread can entirely be assigned to random measurement uncertainties. For our assessment, the devolatilization reaction 10 is used as this reaction is not overlapping with other reactions. This enabled the extraction of the T_{hm} which is required for the calculation of the confidence ellipses since T_{hm} influences the area and the orientation of the confidence regions (equation 8). The kinetic parameters of the individual replicates of reaction 10 did not project within the confidence region of each other (Figure 5) and therefore, the spread of E and ln(A) cannot be attributed to solely random experimental errors. The slope of a linear regression curve through the 9 replicates is close to the orientation of the confidence ellipses ($\tan\Theta = 1/(RT_{\mathrm{hm}})$).

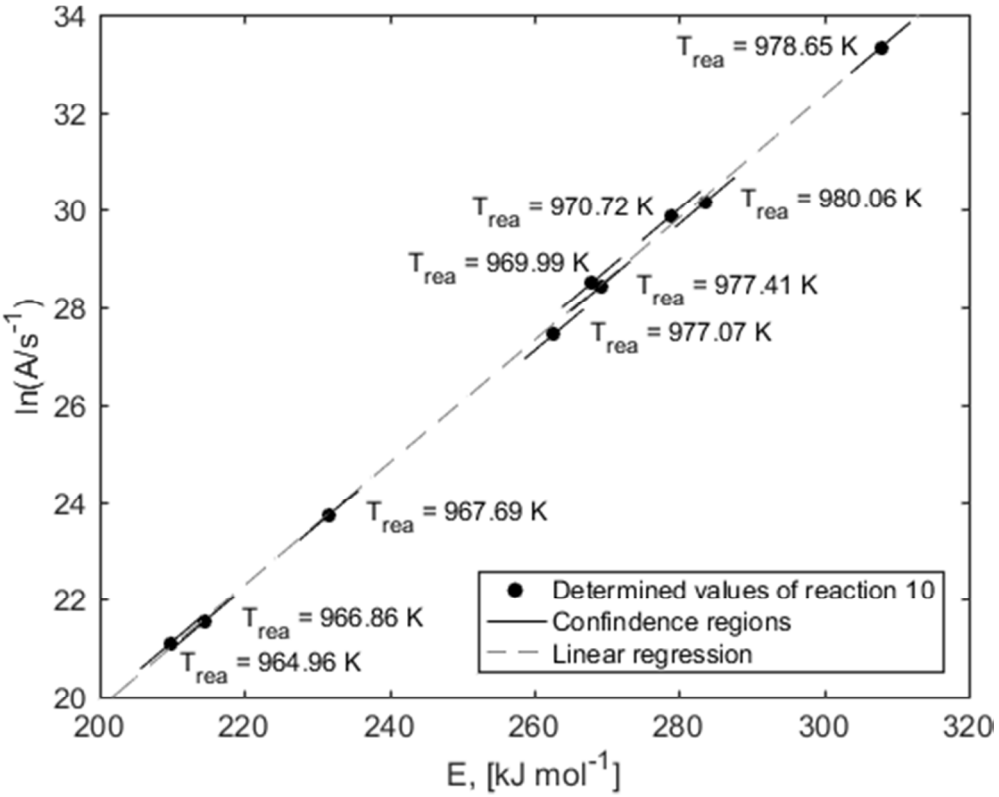

Figure 5: Confidence regions for reaction 10. Values (black dots) of E and A correspond to those of reaction 10 in Figure 4. The black lines represent the ranges of E and A, within which the experimental values can statistically vary in the absence of systematic errors. The orientation of the black lines can be determined from the harmonic mean temperature ($\tan\Theta = 1/(RT_{hm})$) and the length relates to the square-root of the eigenvalues of the variance-covariance matrix [22]. The ellipses appear as a line, since the ratio of λ_1/λ_2 is around 10^4. A linear regression ($R^2 = 0.9990$) is shown to guide the eye. T_{rea} indicates the temperature at which the highest rate of devolatilization occurred. Note that T_{rea} can be significantly different from T_{hm} and the values should not be compared.

4.4 Origin of the apparent kinetic compensation and alternative methods to determine *E* and *A*

The slope of the regression line through the projections of the kinetic data (E, ln(A)) derived from the individual 9 replicates (for reaction 10) is indicative of the deviation of the measured activation energy from the true value of the activation energy by a specific effect [24]. The slope of the regression line corresponding to reaction 10 (Figure 5) can be described as follows:

$$\text{slope} = \frac{1}{RT_{\text{hm}}} \quad (10)$$

with $T_{\text{hm}} = 957$ K. The average harmonic mean temperature of all nine replicates is 959.9 ± 1.13 K (mean ± 1 standard deviation). The harmonic mean temperature is the temperature at which any combination of *E* and *A* on the corresponding regression will yield the same reaction rate constant *k* (eq. 1). A slope of $1/RT_{\text{hm}}$ is indicative of a constant systematic error or a systematic error which varies with temperature [24]. Other errors, e.g. related to catalyst activity, produce different slopes of the linear regression or even exhibit nonlinear behavior and can thus be excluded [24]. Lower reaction temperatures (T_{rea}) generally result in lower absolute values for *E* and *A* (Figure 5) and higher peak temperatures lead to higher pairs of *E* and *A* in a kinetic analysis. However, as long as pairs of *E* and *A* share the same harmonic mean temperature, they will project on the same regression line. Thus, apparent kinetic compensation as observed in our experiments is likely caused by variations of the experimental temperature related to an insufficient precision of the TGA. Repeating the TG experiments with lower heating rates leads to lower values of *E* and *A*, however the values still scatter on the same regression line (Figure 6). Analogously, higher heating rates produce higher values of *E* and *A* on the same regression line (Figure 6). Additionally, the TGA evaluation algorithm returns fewer reactions for experiments with lower heating rates (Figure 6), which might result from less noise in the thermograms and a more precise setting of the temperatures by the TGA. Largest deviations between measured and programmed temperatures were observed at the highest heating rates. Thus, the higher the actual temperature of the experiment, compared to the instrument setting temperature, the higher the deviation of the measured activation energy from the true value of the activation energy. Thus, complementary information of (i) replicate experiments conducted at the same heating rates (Figure 5) and (ii) replicate experiments conducted at different heating rates (Figure 6) revealed that the applied method (TGA measurement and evaluation) resulted in values for *E* and *A* of the combustion of digested sewage sludge, which are generally too high and vary considerably. Even at extremely low temperature ramps like 1 K/min, the deviation of the measured temperature to the programmed temperature is around 4 K.

To further assess the origin of the apparent kinetic compensation in our dataset, two alternative methods to extract the kinetic parameters (E and A) from reaction 10 were applied. As in the previous section, reaction 10 was chosen as it does not overlap with any other devolatilization reaction. Firstly, we applied an unconstraint (model-free) isoconversional integral approach, and secondly, we used the Coats-Redfern method [29]. For the isoconversional method, the objective function (OF_E, equation 11) is minimized to obtain one single, average E over the entire course of the reaction 10 [30]. The activation energy value derived from an average TG curve (black dot, Figure 4) was chosen as an initial value. Minimization is achieved using the function *fminsearch* in Matlab.

$$OF_{\mathrm{E}} = \left| 1 - \frac{\sum_{i=1}^{n} I(E,T_2)B_1}{\sum_{i=1}^{n} I(E,T_1)B_2} \right| \quad (11)$$

With $I(E,T) = \int_{T_0}^{T} \exp(-E/(RT))\, dT$, B_1 and B_2 are two heating rates with $B_1 \neq B_2$ and the sums from 1 to n (n = 100) cover the whole temperature range at which reaction 10 occurred. $I(E,T)$ was integrated numerically. Through minimization, we obtain the activation energy E, which best describes the reaction occurring at both heating rates. Similarly, A was determined by minimization of the objective function OF_A (eq. 12). $\log_{10}(A)$ was used as a parameter for the minimization, which was achieved by the function *fminbnd* in Matlab with $0 < \log_{10}(A) < 50$ as constraints. The constrains were selected based on expected values for A.

$$OF_{\mathrm{A}} = 1 - \frac{\sum \log_{10} \left| \frac{g(\alpha)B_1}{I(E,T_1)} - 10^{log10(A)} \right|}{\sum \log_{10} \left| \frac{g(\alpha)B_2}{I(E,T_2)} - 10^{log10(A)} \right|} \quad (12)$$

The function $g(\alpha)$ represents the integrated reaction model (see eq. 3). The isoconversional method was evaluated using modeled data and found to reproduce kinetic parameters with errors less than 1.0% (Figure S3). For the analysis, only the TG data from sludge sample P1 above 600 °C is used to only include reaction 10. Equation 10 is minimized to obtain E of reaction 10. Values of E range from 242 kJ/mol to 344 kJ/mol, and are slightly higher compared to those determined by the TGA evaluation algorithm (Figure 7). Minimizing OF_A yields the corresponding values for A. A first-order model ($g(\alpha) =$

$-\ln(1-\alpha)$) was chosen to be comparable to the TGA evaluation algorithm. Obtained kinetic parameters scatter on the same line as the results from the TGA evaluation algorithm and even overlap to some extent (Figure 7). One assumption of the TGA evaluation algorithm is that any detected first-order reaction reaches the maximal rate of decomposition at $W(t) = 1 - \mathrm{e}^{-1} = 63\%$ [18]. In contrast, the median in the experimental data at which reaction 10 reaches its maximal rate of decomposition is at $W(t) = 75\%$ with values ranging from 65% to 78%. This is determined via $W(t)$ at the maximum of the first derivation of $W(t)$. Although all combinations of E and A on the linear regression line describe the same thermal conversion which share a common harmonic mean temperature, higher values for E and A shift the maximum conversion to higher temperatures (and higher $W(t)$). Varying the maximal decomposition rates from 65% to 78%, however, did not significantly improve the results from the TGA evaluation algorithm (data not shown). The isoconversional integral does not contain a specific criterion for the maximal rate of conversion, which is automatically adjusted depending on the dataset. As the maximum rate of decomposition occurs at higher values of $W(t)$ than 63%, the application of the isoconversional integral method results in higher pairs of E and A compared to the pairs determined by the TGA evaluation algorithm.

The graphical Coats-Redfern method was one of the first methods to determine E from constant heating rate experiments [29]. Although the method is associated with a considerable uncertainty [19, 31], it was used to reveal the dependence of E on the evaluation method. When plotting $\log_{10}\left(\frac{-1-(1-B)^{1-n}}{T^2(1-n)}\right)$ against $1/T$ with the reaction order n, a first-order reaction should yield a straight line, where the slope relates to E and the y-axis intercept can be used to calculate A [29]. The results corresponding to a first-order reaction model project well on the extension of the results of the TGA evaluation algorithm and the results of the isoconversional method (Figure 7). This implies that all three methods yield the same kinetic rate constant k (compare eq. 1) for the harmonic mean temperature T_{hm}, but assign different E and A. The selection of an inappropriate reaction model, may result in strongly varying E and A [21]. Higher weight change rates towards the end of the reaction are indicative of either (i) higher values of E and A (but still scattering on

the regression with a constant harmonic mean temperature) or (ii) a n-th order reaction model with $n < 1$. Therefore, we evaluated a pseudo 0.5-order reaction model ($f(\alpha) = (1-\alpha)^{\frac{1}{2}}$) for the Coats-Redfern method [29]. This resulted is a significantly reduced spread of values of *A* and *E* (Figure 7) and all values projected within the confidence regions of each other (Figure 7 and Figure S4). These results suggested that the apparent kinetic compensation may also have resulted from choosing an inappropriate reaction model. Although fitting results may improve when using reaction orders $n \neq 1$, results based on different reaction orders can hardly be compared anymore. The determination of kinetic triplets based on reaction orders $n \neq 1$ is therefore of limited use [18].

Thus, the first-order reaction model used in the TGA evaluation algorithm may not be appropriate and may result in an apparent kinetic compensation. However, although different analysis techniques (or instruments used to record TG data [32]) result in different kinetic parameters for the same reaction, extracted *A* and *E* values will project on the same straight line on a Constable plot. The absolute values of *E* and *A* remain uncertain, but their ratios can be used to identify reactions, as demonstrated in the following section.

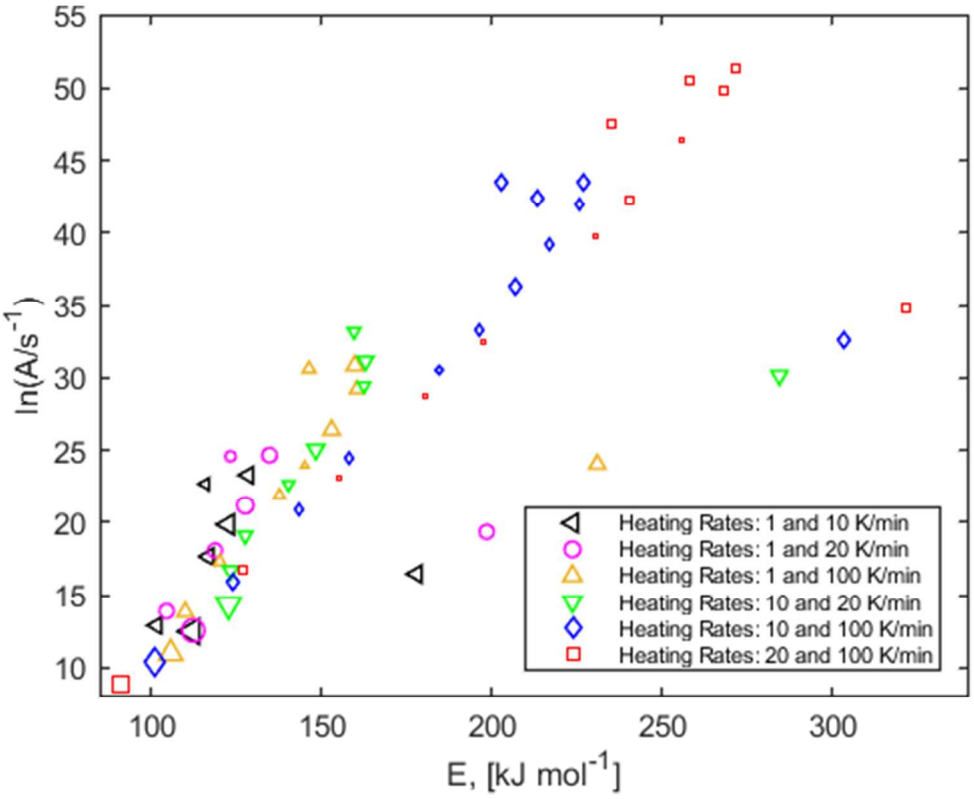

Figure 6: Activation energy (E) and pre-exponential factor (A) extracted from experiments conducted with different heating rates. Higher heating rates generally lead to higher values of E and A for the same conversions. Also higher heating rates tend to results in more reactions returned by the evaluation algorithm.

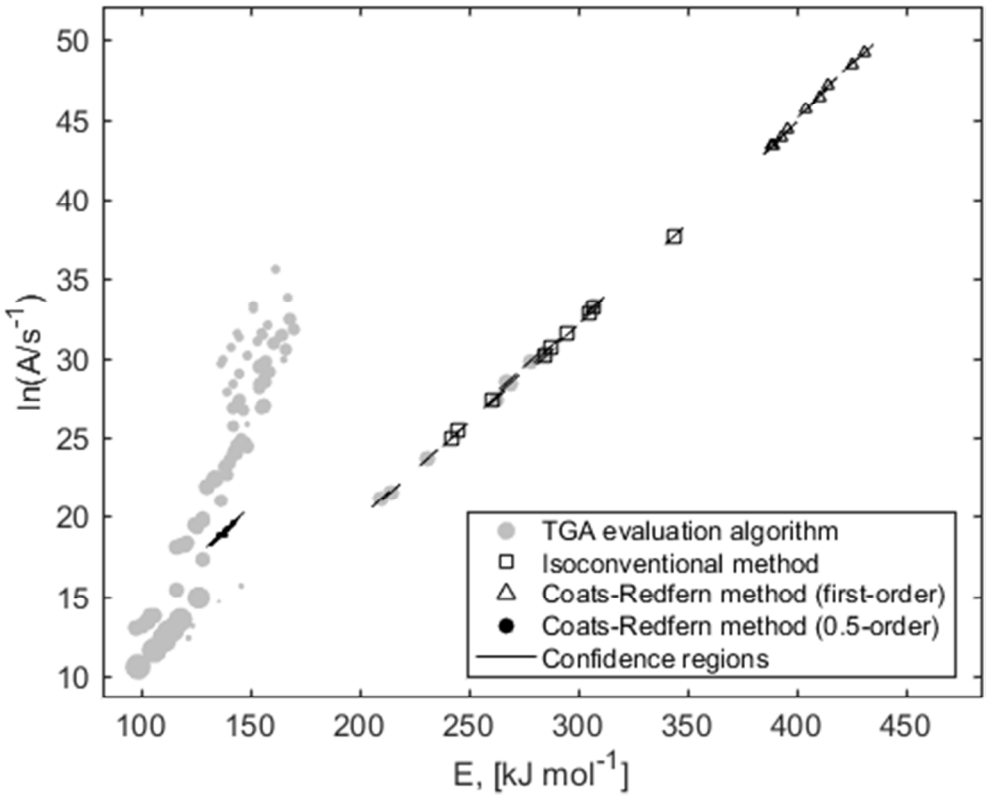

Figure 7: Constable plot derived using the TGA evaluation algorithm (grey dots). *E* and *A* for reaction 10 of the P1 dataset were additionally calculated using (i) the isoconversional integral method (empty rectangles), (ii) the Coats-Redfern method first-order reaction (empty triangles), and (iii) the Coats-Redfern method 0.5-order reaction (black dots). The confidence intervals are given as black lines.

4.5 Assigning identified reactions to the combustion of specific compounds

In the previous section, we showed that different evaluation methods yield different pairs of *E* and *A* for the same dataset, but all project on a straight line in a Constable plot.

Based on the following four criteria, specific compounds were assigned to the identified reactions: (i) the kinetic parameters (*E* and *A*) of the compound must project on the extension of the regression line of the reaction of interest, (ii) the reaction must occur at comparable temperatures, (iii) the reaction order must be one, and (iv) the compound must suit to the context. To evaluate whether the kinetic parameters of selected model compounds project on the extensions of a reaction of interest, the slope of the linear regression through the projections of the kinetic parameters of the reaction of interest is compared to the

slope of a straight line defined by the y-axis intercept of the linear regression and the projection of the kinetic data of the specific compound (eq. 13).

$$\text{slope} = \frac{E_x}{\ln(A_x/s^{-1}) - A_0} \quad (13)$$

E_x (here in kJ/mol for convenience) and A_x are experimental or literature values of E and A, respectively. A_0 is the y-axis intercept of a linear regression through all replicates associated with **reaction 1** to **10** from this study, thus different for each reaction. The linear regressions are represented by the grey lines in Figure 8. Selected studies report standard deviations or ranges for E and A ((Table 3), Figure 8, Figure 9, error bars). Standard deviations of activation energies typically range around 5%, e.g. [33-34] and we therefore assumed an uncertainty of $\pm$ 5% in the slope, if no standard deviations were provided. If the slopes of the identified reactions and the slopes constructed for the reaction of reference compounds overlapped considering their uncertainties, the reaction of interest were assigned the respective reference compound.

Reaction 10, which again is used as an example, most likely represents the conversion of calcium carbonate to calcium oxide and carbon dioxide ($CaCO_3$ -> CaO + CO_2) [10]. A previous study used an isoconversional method to determine the kinetic parameters of the conversion of calcium carbonate (calcite) [34]. The reaction related to the conversion of calcite projects on the extension of the regression line of the nine replicate measurements of **reaction 10** (Figure 8). The projection of the conversion reaction of calcite on the extension of the regression line through the nine replicates of reaction 10 implies that the kinetic parameters of the calcite conversion share the same kinetic constant (k) as the extracted parameters of **reaction 10** at a common harmonic mean temperature (957 K). The weight loss of pure calcite conversion occurs between 900 and 1200 K [34], the harmonic mean temperature in the present study is 957 K. The study by Rodriguez-Navarro et al. was performed with pure calcite crystals [34]. Thus, the lower temperature obtained in our study may be explained by differences in the matrix and different size and crystallinity of the calcite. Furthermore, the kinetic parameters of the calcite conversion ($E = 179.90 \pm$

10 kJ/mol and $\ln(A/s^{-1}) = 17.46$) [34] match those of **reaction 10** determined from experiments with heating rates of 1 and 10 K/min ($E = 177.95$ kJ/mol and $\ln(A/s^{-1}) = 16.47$) very well (Figure 6). For **reaction 10** $A_0 = -5.35$ was determined which leads to slopes (each pair of E_x and A_x results in a slightly different slope) of 7.96 ± 0.03 (Figure 9). A straight line defined by A_0 and the projections of E and A for the conversion of calcite [34] results in a slope of 7.89 ± 0.44 (Figure 9) overlapping with the slope of the regression line considering the respective standard deviations. We thus assigned **reaction 10** to the thermal conversion of calcite to calcium oxide.

Yang et al. suggested to treat the pyrolysis of any biomass as a superposition of the pyrolysis of cellulose, hemicellulose and lignin [35]. Cellulose, a polymer derived from β-D-glucose molecules may only be degraded incompletely during anaerobic digestion [36] and its presence in the sludge is mainly related to toilet paper [7-8]. The weight loss related to the combustion of cellulose, usually referred to as $nC_6H_{12}O_6 + 6nO_2 \rightarrow 6nCO_2 + 6nH_2O$ is best described by a series of reactions, where charring, volatilization, char oxidation and volatile oxidation can be distinguished [37]. These four processes may all occur at different stages of the TG experiment, although volatile oxidation cannot be observed in our experiments, as this either occurs in the furnace above the balance or the volatiles escape from the TGA without further oxidation. We assumed that the conversion of cellulose is best described by multiple first-order reactions. The same applies to other biopolymers (see [37-38] for a more detailed discussion on the 'combustion' of biopolymers), and kinetic data for multiple reactions were considered when available.

Hemicelluloses are amorphous polymers made from a variety of natural monomers [35]. Lignin is a phenolic polymer made from p-hydroxyphenylpropanoid monomers which are cross-linked via C-O and C-O-C bonds [39]. It is very resistant to enzymatic and chemical degradation [40], thus likely present in digested sewage sludge [7, 9]. Xylan is a specific type of hemicellulose, derived from hardwood [37] and alginate is a good surrogate for cell biomass [41], which represents a significant fraction of the digested sludge [1]. These five organic compounds (cellulose, hemicellulose, lignin, xylan, and alginate) and calcite, are thus considered as important reference compounds to explain the combustion of sewage sludge (Table 3).

Reactions of selected reference compounds, reactions identified by Hernández et al. and the reactions identified in this study are displayed on the same Constable plot (Figure 8) [17]. Error bars indicate two standard deviations of the activation energy wherever available. The grey lines are extrapolations of the linear regressions from to identified reactions of our dataset. The slopes of the linear regressions and the slopes of the straight lines defined by A_0 and E and A from the literature are given in Figure 9.

The combustion of hemicellulose and xylan [42] are split in two reactions and the first reaction (open upward pointing triangle and open star Figure 8) project close to the extension of reaction 2 of our study. The slight mismatch (Figure 9) between the data from the literature and our results may be explained by evaporation of residual water from the sludge samples at this stage of the experiment [12].

The kinetic parameters determined for alginate (right pointing triangle, [33]) project on the extension of our **reaction 3** (Figure 9). Also the first reaction of the combustion of sewage sludge identified by Hernandez et al. [17] projects on the same extension. The harmonic mean temperature of **reaction 3** is 563 K, Hernandez et al. [17] report 566 K for their reaction 1 and the combustion of alginate occurs between 473 K and 573 K. Thus, **reaction** 3 very well fits to the combustion of alginate.

The second combustion reaction of xylan (black, filled star, [42]), the cellulose volatilization (red, open square, [43]) and the oxidation of volatiles derived from cellulose (magenta, open square, [44]) project on the extension **reaction 6**. The latter ones would not be detected in our TG experiments and are thus not considered in our evaluation. Also the third reaction of Hernandez et al. [17] project on the same extension. The slope of **reaction 6** projects within the standard deviations of the identified reference reactions (Figure 9) and we therefore assigned **reaction 6** to the second combustion reaction of xylan.

The cellulose reaction 1 (black, open square, [45]), and the second reaction of hemicellulose (filled triangle, [42]) project on the extension of our **reaction 7**. The fourth reaction of Hernandez et al. [17] also projects on this extension. The authors report a slightly lower temperature for this reaction (692 K compared to 751 K for our experiments). The slopes of cellulose reaction 1 and the fourth reaction of Hernandez et al. [17]

project within the standard deviations of the slope of **reaction 7**. The slope of the hemicellulose reaction 2 is slightly lower, but still is within the standard deviation of the slope of **reaction 7**. Thus, **reaction 7** is associated with the cellulose reaction 1, hemicellulose reaction 2 and the fourth reaction of Hernandez et al. [17].

The oxidation of char derived from cellulose (blue, open square, [46]) projects on the extension of **reaction 8**. The reported temperature of the oxidation of char derived from cellulose is roughly 80 K lower compared to the determined harmonic mean temperature of our reaction. The temperature deviation likely originates from the fact that Branca et al. [46] ran experiments with pure cellulose and we consider cellulose as a model substance to describe an apparent reaction that represents the oxidation of char derived from cellulose like material. The slope of the cellulose char oxidation projects within the 75th percentiles of the slopes of **reaction 8** and we thus assigned **reaction 8** to the oxidation of char derived from cellulose like substances.

The second reaction of cellulose (black, filled square, [45]) and lignin (black, filled diamond, [45]) project on the extension of **reaction 9**, which is the reaction with the largest weight loss. Also the fifth reaction reported by Hernandez et al. [17] falls on the trend defined by the **reaction 9**. The upper end of the combustion temperatures for lignin and cellulose are reported at 722 K and 755 K, respectively. This is in good agreement with the temperature obtained from our experiments (763 K) and reported by Hernandez et al. [17] (748 K). The slopes of both reference reactions and the fifth reaction reported by Hernandez et al. [17] fall within the standard deviation of the slope of **reaction 9. Reaction 9** is therefore assigned to the second reactions of cellulose and lignin [45].

The lignin reaction 1 (open diamond) projects between the extensions of **reactions 8** and **9** and an assignment of this reaction to a specific compound remains ambiguous. The thermal decomposition of calcite [10] clearly matches **reaction 10**, as outlined above.

The regression line of **reaction 4** aligns well with the second reaction reported by Hernandez et al. [17], however, no suitable reference compound for this reaction was found in the literature. The same also applies for **reactions 1** and **5**. Reaction 1 is likely related to the evaporation of residual water, tightly bound to the sludge matrix. Reactions 4 and 5 may be explained by the decomposition of cell tissue and extra-cellular polymeric substances (EPS), which are both present in digested sludge but are only represented by the decomposition of alginate with 8%. However, as the kinetic parameters of the thermal decomposition of cell tissue and EPS were not available, the assignment of reactions 4 and 5 to these compounds remains speculative.

E and *A* of sewage sludge combustion reported by Hernandez et al. are generally higher compared to the respective values obtained in this study, likely caused by higher heating rates [17]. Both sludge samples (present study and Hernandez et al. [17]) refer to digested sludge but still may differ in their compositions.

The weight loss (total conversion) calculated from the kinetic parameters derived from the TGA evaluation algorithm is in excellent agreement with the three sections of the thermogram identified in Figure 1. Combustion phase 1 included roughly 50% of the total conversion (weight loss). Reaction 1 to 7, including the devolatilization of alginate, hemicellulose, xylan, the volatilization of cellulose, the burning of volatiles derived from cellulose, and the first of two combustion reactions of cellulose all contribute to the first combustion phase and combine also to 50% of the total conversion (Table 2). Combustion phase 2 accounts for about 40% of the total conversion (Figure 1). This is in good agreement to the 37% resulting from reactions 8 (cellulose char oxidation) and reaction 9 (lignin char oxidation). The remaining 10% of the converted weight are assigned to phase 3 and correspond well to the 11% found for reaction 10 (conversion of calcite) (Table 2).

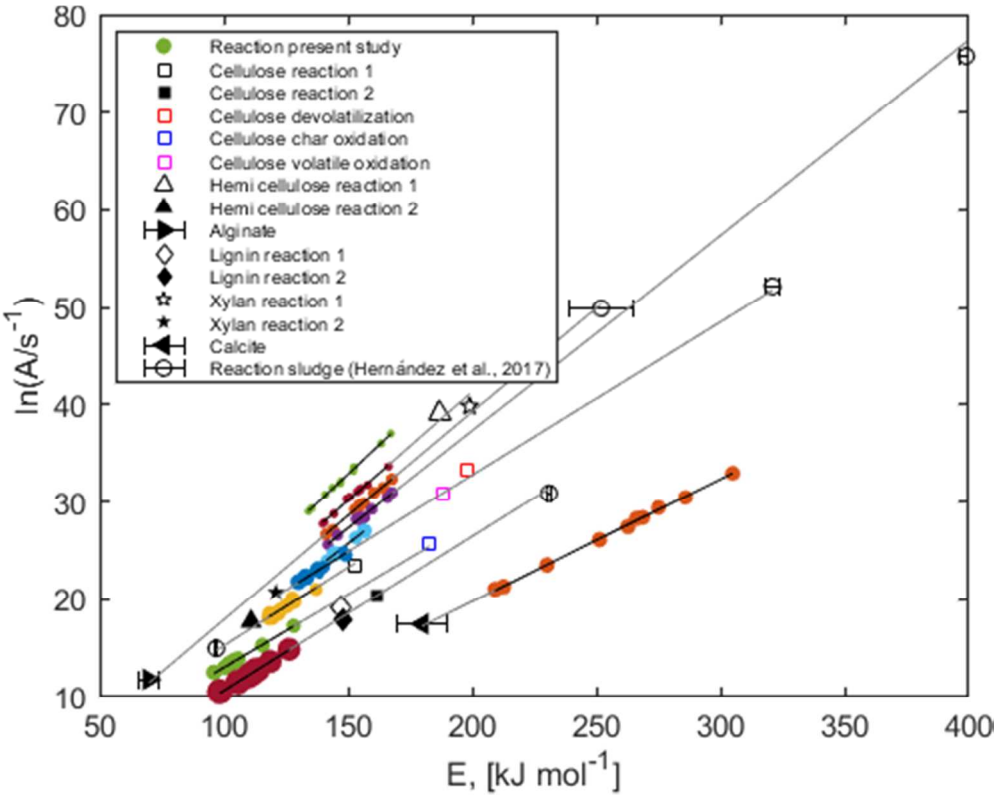

Figure 8: Constable plot of results from i) this study (colored dots), ii) from Hernandez et al. [17] (black circles) and iii) from selected reference compounds (other symbols). The conversion reactions of cellulose are plotted as squares (open, filled, different colors), other reference substances are shown in other black symbols. Two types of lines are shown: (i) a linear regression through each reaction in black (compare Figure 5) and (ii) gray lines, suggesting associations between the reference reactions and the reactions of the present study. All reactions are listed in Table 2 and Table 3. Note that the sorting of the reactions changed compared to Figure 3 and each color is now associated with one of the reactions rather than an experimental replicate.

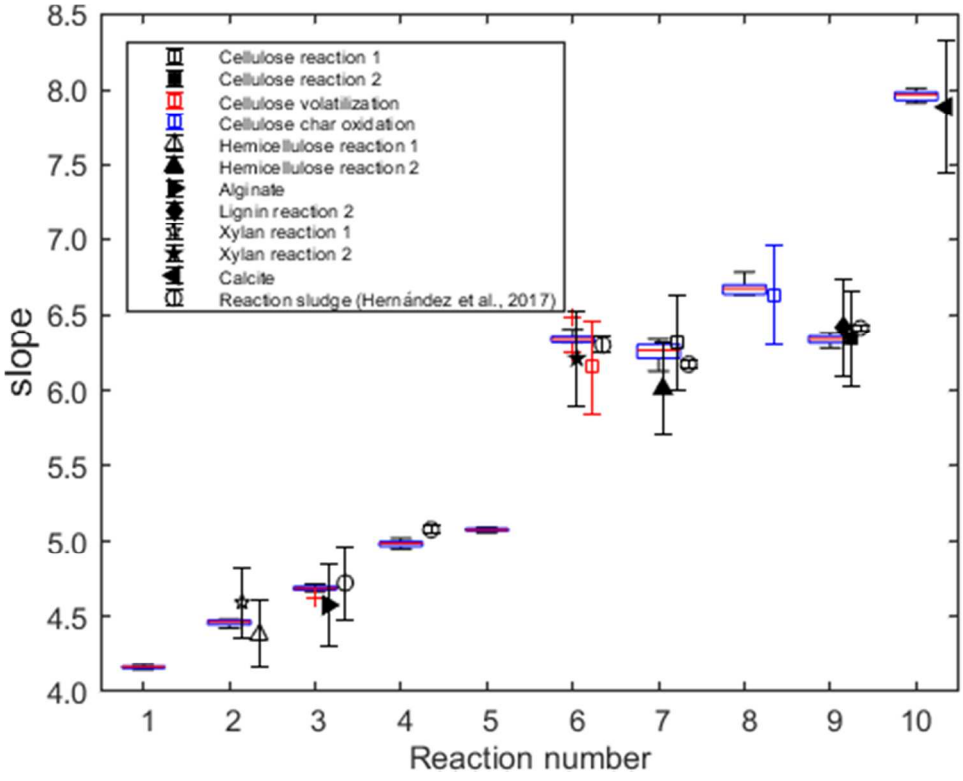

Figure 9: Boxplot of the slopes of E and A for reactions 1 to 10. The red lines represent the median values, the blue boxes the 25th and 75th percentiles, the whiskers the extreme values for each reaction ($n = 9$) and the red plus the outliers. Slopes of reference compounds (see text for the calculation of the slopes) from the literature are also shown using black symbols, colored squares for specific reactions of cellulose. These values are displayed next to the identified reactions. The same data are shown in a Constable plot (Figure 8).

Table 3: Kinetic parameters (E (activation energy), A (pre-exponential factor), of different organic compounds and of other reactions found for sewage sludge combustion. In each case, the reaction order is one or close to one $0.95 < n < 1.05$. *The decomposition of this substance consists of two peak areas which were determined in the same experiment.

Substance	E, [kJ/mol]	$\ln(A/s^{-1})$	Reported Peak temperature or temperature range, [K]	Reference
Cellulose*	153 & 162	23.44 & 20.43	499.15 – 578.15 & 608.15 – 755.15	[45]
Cellulose Volatilization	198	33.36	ca. 623	[43]
Cellulose volatile oxidation	188	30.86	Not available.	[44]
Char oxidation	183	25.64	700 - 730	[46]
Alginate	69.63 ± 4.07	11.82 ± 1.01	473.15 - 573.15	[33]
Hemicellulose*	187 & 111	39.10 & 17.71	Not available.	[42]
Lignin*	147 & 148	19.09 & 17.94	560.15 – 579.15 & 579.15 - 722.15	[45]
Xylan*	199 & 121	39.79 & 20.70	Not available.	[42]
Calcite	179.9 ± ca. 10	17.46	ca. 1100	[34]
Sewage sludge combustion: Reaction 1	252.1 ± 12.9	49.91	566.15	[17]
Sewage sludge combustion: Reaction 2	399.8 ± 2.3	75.67	607.15	[17]
Sewage sludge combustion: Reaction 3	97.0 ± 0.5	14.95	607.15	[17]
Sewage sludge combustion: Reaction 4	321.9 ± 2.6	52.21	692.15	[17]
Sewage sludge combustion: Reaction 5	231.6 ± 0.7	30.82	748.15	[17]

4.6 Relating the weight loss associated with the conversion of reference compounds to the weight loss associated with individual reactions derived from TG analyses.

For selected substances the conversion occurs via multiple reactions or the conversion of several substances contribute to the same reaction identified through the TGA evaluation algorithm. Therefore, we set up a linear system of equations to balance the reactions, $M\vec{x} = \overrightarrow{f_0}$ (equation 14). The matrix M contains information on whether the reaction of certain reference compound overlaps with a specific reaction identified by the TGA evaluation algorithm. For simplicity, we assume that overlapping reactions of reference compounds contribute equally to the total weight loss of a specific reaction identified by the TGA algorithm and, therefore, a one in the matrix represents an (equal) overlap of a certain reference compound (columns) with a reaction identified by the TGA algorithm. The reference compounds are ordered in the following way (columns from left to right): cellulose, hemicellulose, xylan, lignin, alginate, calcite. The vector $\overrightarrow{f_0}$ represents the weight fractions associated with the individual reactions identified by the TGA evaluation algorithm. M and $\overrightarrow{f_0}$ are linked via the vector $\vec{x}$, which describes the weight fraction associated with a specific model compound with respect to the individual reactions identified by the TGA evaluation algorithm.

$$\begin{bmatrix} 0 & 1 & 1 & 0 & 0 & 0 \\ 1 & 0 & 1 & 0 & 0 & 0 \\ 1 & 1 & 0 & 0 & 0 & 0 \\ 1 & 0 & 0 & 0 & 0 & 0 \\ 1 & 0 & 0 & 1 & 0 & 0 \\ 0 & 0 & 0 & 0 & 1 & 0 \\ 0 & 0 & 0 & 0 & 0 & 1 \end{bmatrix} \begin{bmatrix} x_1 \\ x_2 \\ x_3 \\ x_4 \\ x_5 \\ x_6 \end{bmatrix} = \begin{bmatrix} f_0(R_2) \\ f_0(R_6) \\ f_0(R_7) \\ f_0(R_8) \\ f_0(R_9) \\ f_0(R_3) \\ f_0(R_{10}) \end{bmatrix} \quad (14)$$

The linear system of equations ($M\vec{x} = \overrightarrow{f_0}$) is solved using Matlab. Rows 6 and 7, corresponding to reactions 3 and 10, respectively, only contain a single ONE. Therefore $\vec{x}_6 = f_0(R_3)$ and $\vec{x}_7 = f_0(R_{10})$. Thus, the reactions 3 and 10 directly correspond to the burning of alginate (reaction 3) and conversion of calcite (reaction 10), respectively. In the case of the other reference substances, their contribution to the total weight loss observed during the TGA experiments corresponds to the sum of the respective column

vector of M times $\overrightarrow{x^T}$ ($M\overrightarrow{x^T}$). Results suggest that cellulose (36%) and lignin (20%) dominate the observed weight loss. Furthermore, the conversion of hemicellulose (6%), alginate (8%) and calcite (11%) contributes with comparable amounts to the total weight loss (Figure 10). Xylan, plays a minor role with respect to the weight loss observed in the TGA experiments. The reactions of the six reference compounds explain more than 80% of the total weight loss obtained from TGA experiments. The conversion of calcite can be compared to the difference in inorganic carbon (IC) contents between sludge and ash, assuming that the loss of IC is associated with calcite ($CaCO_3$). The IC content in the sludge was 1.85% and 1.13% in the ash, corresponding to 0.34% when normalized to an ash content of 30%. The loss of IC thus amounted to 1.5% which translates to 12.5% CaCO3 in excellent agreement with the 11.4% calculated from the TGA results. In a recent study, the cellulose content in WWTP influents was estimated to 35% - 40% of the total suspended solids [7] and only incomplete degradation of cellulose is expected during conventional wastewater and sludge treatment [7, 9]. This study suggested that ~ 50% of cellulose is degraded during aerobic treatment as well as during anaerobic sludge digestion. Considering that the majority of chemical oxygen demand (COD) fed into the anaerobic digestion in our pilot WWTP originates from the primary sludge, and taking into account that our pilot anaerobic digester likely results in less efficient degradation of COD, a cellulose fraction of 35% of the TSS seems reasonable. Higher ratios of cellulose to lignin (1.8) from our pilot digester compared to reported ratios of 0.4 [7, 9] further support the hypothesis of a lower degree of cellulose degradation, in line with the less complex sludge composition (fewer reactions identified by the TG analyses) of our digested sludge compared to digested sludge from full-scale digesters.

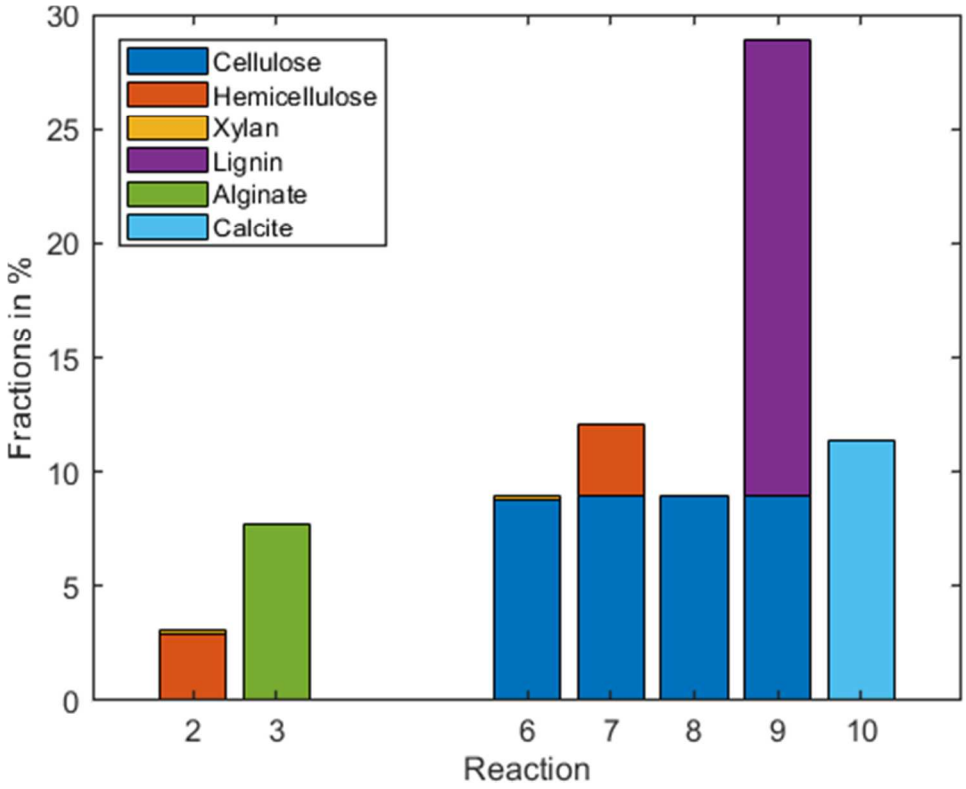

Figure 10: Reactions identified by the TGA evaluation algorithm (1-10) versus the fractions of reference compounds assigned to specific reactions. No specific compounds were assigned to reactions 1, 4 and 5, but the weight loss of the remaining reactions where reference compounds were identified accounts for more than 80% of the total weight loss observed during the TGA experiments.

5 Conclusions

The combustion of digested sewage sludge can be described by ten first order reactions, which are partly overlapping. Kinetic parameters of replicate experiments exhibited an apparent kinetic compensation effect, likely caused by slight variations of the temperature setting of the TGA instrument. Furthermore, a comparison of results obtained from different evaluation methods revealed a substantial impact of the specific evaluation method on the determined absolute values of activation energy (E) and pre-exponential factor (A). However, on a Constable diagram E and A of replicate experiments for a specific reaction always plot on a straight line which is characteristic for the respective reaction. The reactions identified through the TG analysis of digested sewage sludge were assigned to the following reactions of reference

compounds reported in the literature: lignin, cellulose, hemicellulose, alginate, xylan and calcite. The total weight loss observed during the combustion of digested sewage sludge is dominated by cellulose and lignin devolatilization and char burning which contribute about 35% (cellulose) and 20% (lignin) of the total conversion. The conversion of all reference compounds explains more than 80% of the weight loss of digested sewage sludge observed in our TG experiments. Our approach, thus, offers the possibility to assess the speciation of combustible in digested (and possibly also activated) sludge, which may be relevant for an evaluation of the impacts and removal of cellulose in wastewater treatment plants.

6 Acknowledgements.

The authors like to acknowledge financial support from the Swiss National Science Foundation under the project 5221.01038.001. Also, the authors like to acknowledge support in the laboratory from Agnieszka Kierzkowska (ETH Zurich) and Brian Sinnet (Eawag), and Felix Donat for helpful suggestions concerning kinetic compensation.

Supporting Information. Contains the derivation of equation 4 and 4 Figures on the validation of the applied evaluation methods.

7 References

1. Metcalf; Eddy, I.; Tchobanoglous, G.; Burton, F.; Stensel, H. D., *Wastewater Engineering: Treatment and Reuse*. McGraw-Hill Education: 2002.

2. Kelessidis, A.; Stasinakis, A. S., Comparative study of the methods used for treatment and final disposal of sewage sludge in European countries. *Waste Management* **2012,** *32* (6), 1186-1195.

3. Laube, A.; Vonplon, A., Klärschlammentsorgung in der Schweiz, Mengen- und Kapazitätserhebung. *BUWAL* **2004**.

4. Wiechmann, B.; Claudia, D.; Christian, K.; Simone, B.; Ines, V.; Andrea, R., Sewage Sludge Management in Germany. *Umweltbundesamt Deutschland, January* **2015**.

5. Werther, J.; Ogada, T., Sewage sludge combustion. *Progress in Energy and Combustion Science* **1999,** *25* (1), 55-116.

6. Donatello, S.; Cheeseman, C. R., Recycling and recovery routes for incinerated sewage sludge ash (ISSA): A review. *Waste Management* **2013,** *33* (11), 2328-2340.

7. Ruiken, C. J.; Breuer, G.; Klaversma, E.; Santiago, T.; van Loosdrecht, M. C. M., Sieving wastewater – Cellulose recovery, economic and energy evaluation. *Water Research* **2013,** *47* (1), 43-48.

8. Chen, R.; Nie, Y.; Kato, H.; Wu, J.; Utashiro, T.; Lu, J.; Yue, S.; Jiang, H.; Zhang, L.; Li, Y.-Y., Methanogenic degradation of toilet-paper cellulose upon sewage treatment in an anaerobic membrane bioreactor at room temperature. *Bioresource Technology* **2017,** *228*, 69-76.

9. Verachtert, H.; Ramasamy, K.; Meyers, M.; Bevers, J., Investigations on cellulose biodegradation in activated sludge plants. *Journal of Applied Bacteriology* **1982,** *52* (2), 185-190.

10. Barneto, A. G.; Carmona, J. A.; Alfonso, J. E. M.; Blanco, J. D., Kinetic models based in biomass components for the combustion and pyrolysis of sewage sludge and its compost. *Journal of Analytical and Applied Pyrolysis* **2009,** *86* (1), 108-114.

11. Chen, X.; Jeyaseelan, S., Study of Sewage Sludge Pyrolysis Mechanism and Mathematical Modeling. *Journal of Environmental Engineering* **2001,** *127* (7), 585-593.

12. Conesa, J. A.; Marcilla, A.; Moral, R.; Moreno-Caselles, J.; Perez-Espinosa, A., Evolution of gases in the primary pyrolysis of different sewage sludges. *Thermochimica Acta* **1998,** *313* (1), 63-73.

13. Conesa, J. A.; Marcilla, A.; Prats, D.; Rodriguez-Pastor, M., KINETIC STUDY OF THE PYROLYSIS OF SEWAGE SLUDGE. *Waste Management & Research* **1997,** *15* (3), 293-305.

14. Folgueras, M. B.; Alonso, M.; Díaz, R. M., Influence of sewage sludge treatment on pyrolysis and combustion of dry sludge. *Energy* **2013,** *55*, 426-435.

15. Hayhurst, A. N., The kinetics of the pyrolysis or devolatilisation of sewage sludge and other solid fuels. *Combustion and Flame* **2013,** *160* (1), 138-144.

16. Scott; Dennis; Davidson; Hayhurst, Thermogravimetric measurements of the kinetics of pyrolysis of dried sewage sludge. *Fuel* **2006,** *85* (9), 1248-1253.

17. Hernández, A. B.; Okonta, F.; Freeman, N., Thermal decomposition of sewage sludge under N2, CO2 and air: Gas characterization and kinetic analysis. *Journal of Environmental Management* **2017,** *196*, 560-568.

18. Scott; Dennis; Davidson; Hayhurst, An algorithm for determining the kinetics of devolatilisation of complex solid fuels from thermogravimetric experiments. *Chemical Engineering Science* **2006,** *61* (8), 2339-2348.

19. Vyazovkin, S.; Burnham, A. K.; Criado, J. M.; Pérez-Maqueda, L. A.; Popescu, C.; Sbirrazzuoli, N., ICTAC Kinetics Committee recommendations for performing kinetic computations on thermal analysis data. *Thermochimica Acta* **2011,** *520* (1–2), 1-19.

20. Burnham, A. K., *GLOBAL CHEMICAL KINETICS OF FOSSIL FUELS*. Springer: 2017.

21. Vyazovkin, S.; Wight, C. A., Model-free and model-fitting approaches to kinetic analysis of isothermal and nonisothermal data. *Thermochimica Acta* **1999,** *340–341*, 53-68.

22. Barrie, P. J., The mathematical origins of the kinetic compensation effect: 1. the effect of random experimental errors. *Physical Chemistry Chemical Physics* **2012,** *14* (1), 318-326.

23. Liu, L.; Guo, Q.-X., Isokinetic Relationship, Isoequilibrium Relationship, and Enthalpy−Entropy Compensation. *Chemical Reviews* **2001,** *101* (3), 673-696.

24. Barrie, P. J., The mathematical origins of the kinetic compensation effect: 2. the effect of systematic errors. *Physical Chemistry Chemical Physics* **2012,** *14* (1), 327-336.

25. Krug, R.; Hunter, W.; Grieger, R., Enthalpy-entropy compensation. 2. Separation of the chemical from the statistical effect. *The Journal of Physical Chemistry* **1976,** *80* (21), 2341-2351.

26. Petersen, R. C.; Markgraf, J. H.; Ross, S. D., Solvent Effects in the Decomposition of 1,1'-Diphenylazoethane and 2,2'-Azobis-(2-methylpropionitrile). *Journal of the American Chemical Society* **1961,** *83* (18), 3819-3823.

27. Draper, N. R.; Smith, H., Applied Regression Analysis. In *Applied Regression Analysis*, John Wiley & Sons, Inc.: 1998.

28. Glantz, S.; Slinker, B., *Primer of Applied Regression & Analysis of Variance*. McGraw-Hill Education: 2000.

29. Coats, A. W.; Redfern, J. P., Kinetic Parameters from Thermogravimetric Data. *Nature* **1964,** *201* (4914), 68-69.

30. Vyazovkin, S.; Dollimore, D., Linear and Nonlinear Procedures in Isoconversional Computations of the Activation Energy of Nonisothermal Reactions in Solids. *Journal of Chemical Information and Computer Sciences* **1996,** *36* (1), 42-45.

31. Brown, M. E.; Maciejewski, M.; Vyazovkin, S.; Nomen, R.; Sempere, J.; Burnham, A.; Opfermann, J.; Strey, R.; Anderson, H. L.; Kemmler, A.; Keuleers, R.; Janssens, J.; Desseyn, H. O.; Li, C.-R.; Tang, T. B.; Roduit, B.; Malek, J.; Mitsuhashi, T., Computational aspects of kinetic analysis: Part A: The ICTAC kinetics project-data, methods and results. *Thermochimica Acta* **2000,** *355* (1–2), 125-143.

32. Grønli, M.; Antal, M. J.; Várhegyi, G., A Round-Robin Study of Cellulose Pyrolysis Kinetics by Thermogravimetry. *Industrial & Engineering Chemistry Research* **1999,** *38* (6), 2238-2244.

33. Popa, M. I.; Lisa, G.; Aelenei, N., Thermogravimetric characterization of chitosan/alginate microparticles loaded with different drugs. *Polymer Bulletin* **2008,** *61* (4), 481-490.

34. Rodriguez-Navarro, C.; Ruiz-Agudo, E.; Luque, A.; Rodriguez-Navarro, A. B.; Ortega-Huertas, M., Thermal decomposition of calcite: Mechanisms of formation and textural evolution of CaO nanocrystals. *American Mineralogist* **2009,** *94* (4), 578-593.

35. Yang, H.; Yan, R.; Chen, H.; Lee, D. H.; Zheng, C., Characteristics of hemicellulose, cellulose and lignin pyrolysis. *Fuel* **2007,** *86* (12), 1781-1788.

36. Siegert, I.; Banks, C., The effect of volatile fatty acid additions on the anaerobic digestion of cellulose and glucose in batch reactors. *Process Biochemistry* **2005,** *40* (11), 3412-3418.

37. Sullivan, A. L.; Ball, R., Thermal decomposition and combustion chemistry of cellulosic biomass. *Atmospheric Environment* **2012,** *47*, 133-141.

38. Byram, G. M., Combustion of forest fuels. In *Forest fire: control and use*, Davis, K. P., Ed. McGraw-Hill: 1959; pp 61 - 89.

39. Lee, J., Biological conversion of lignocellulosic biomass to ethanol. *Journal of Biotechnology* **1997,** *56* (1), 1-24.

40. Branca, C.; Albano, A.; Di Blasi, C., Critical evaluation of global mechanisms of wood devolatilization. *Thermochimica Acta* **2005,** *429* (2), 133-141.

41. Liu, X. D.; Yu, W. Y.; Zhang, Y.; Xue, W. M.; Yu, W. T.; Xiong, Y.; Ma, X. J.; Chen, Y.; Yuan, Q., Characterization of structure and diffusion behaviour of Ca-alginate beads prepared with external or internal calcium sources. *Journal of Microencapsulation* **2002,** *19* (6), 775-782.

42. Varhegyi, G.; Antal, M. J.; Szekely, T.; Szabo, P., Kinetics of the thermal decomposition of cellulose, hemicellulose, and sugarcane bagasse. *Energy & Fuels* **1989,** *3* (3), 329-335.

43. Antal, M. J., Jr.; Varhegyi, G., Cellulose Pyrolysis Kinetics: The Current State of Knowledge. *Industrial & Engineering Chemistry Research* **1995,** *34* (3), 703-717.

44. Parker, W. J.; LeVan, S. L., Kinetic properties of the components of Douglas-fir and the heat of combustion of their volatile pyrolysis products. *Wood and Fiber Science* **1989,** *21* (3), 289-305.

45. Cheng, K.; Winter, W. T.; Stipanovic, A. J., A modulated-TGA approach to the kinetics of lignocellulosic biomass pyrolysis/combustion. *Polymer Degradation and Stability* **2012,** *97* (9), 1606-1615.

46. Branca, C.; Di Blasi, C., Parallel- and series-reaction mechanisms of wood and char combustion. *Therm Sci* **2004,** *8*, 51-63.